Fabrication of flexible, half printed and all-solid-state asymmetric supercapacitor based on silver decorated reduced graphene oxide

Abd Elhamid M. Abd Elhamid[1,2], Asmaa A. Alamin[1], Ahmed M. Selim[1], Madlin A. Wasfey[1], Mohamed B. Zahran[1,*]

[1] Nanotechnology Lab., Electronics Research Institute, Cairo, 12622, Egypt.

[2] Department of Laser Sciences and Interactions, National Institute of Laser Enhanced Sciences, Cairo University, El-Giza 12613, Egypt.

[*] Corresponding author E-mail addresses: mbazahran@eri.sci.eg (M. B. Zahran)

Abstract: - Flexible supercapacitor (SC) that possess high pulse power and energy density with long lifetime is an essential need for future applications. Moreover, gel polymer liquid-based SC presents many superior advantages over aqueous organic/inorganic electrolytes such as safety, long operation temperature range, solid-state appearance and relatively high voltage window. Therefore, Silver decorated reduced graphene oxide (RGO) coupled with developed (H_3PO_4/PVA/GO/ polyaniline) gel polymer were used to fabricate the SCs, which offers flexibility, durability, safety and ability to apply high scan rate. Influence of different ratios of silver to GO weight on specific capacitance and performance were studied. The SCs were prepared by printing technique (layer by layer) then peeled of the basic plastic substrate. After that, silver thin films were sputtered on both sides of the SCs as the current collectors using a shadow mask as a current collectors. Interestingly, specific capacitance of 164 F/g and energy of 29.5 W/Kg (at 0.25A) were achieved correlated with using H_3PO_4 that is considered to be a weak electrolyte. Moreover, 0.5 ohm represents the smallest electric series resistance that would directly affect the power of the fabricated solid-state SC. The composite was investigated using Raman spectroscopy, TEM and XRD, whereas, The VSP-300 potentiostat/galvanostat was used for extensive electrochemical characterizations of the prepared asymmetric SCs.

Key-Words: - Supercapacitor, flexible, printed, RGO, high scan rate, graphene, gel polymer.

1 Introduction

Energy production and energy storage are one of the main problems facing the whole world those days [1,2]. As the energy production and consumption from fossil fuel is certainly having a severe impact in ecology that produces the greenhouse effect [3]. Therefore, alternative sources with high efficiency are essentially needed [2][4]. In particular, supercapacitor (SCs) raised as a promising candidate for energy storage systems due to their high lifetime and power density [5].

Graphene, the epic 2d carbon material, which has many unique properties such as high theoretical surface area, conductivity, mechanical strength [6]. Graphene was studied extensively in energy storage devices as an active material, additive and [7–10]. It is worth to mention that, one of the main drawbacks of crude RGO is restacking due to strong Van der Waals force, but decoration and function-nalization could retain this problem [11–13].

Most of commercially available SCs use highly porous carbon form and an organic electrolytes with high working voltage window of about 2.7 V. However, liquid electrolyte have major drawbacks such as toxicity, corrosive nature, high vapour pressure, relatively short lifetime, besides the difficulty to fabricate flexible, small , safe device for modern applications and wearable electronics. Accordingly, solid electrolyte such as (ionic liquid, gel polymer (GP) and solid-state electrolyte) offer many advantages such as; environmental friendliness, portability, flexibility, excellent mechanical properties, easy size controlling, reliable, lightweight, wide operation temperature range

[14–17]. Flexible all solid state SCs based on GP electrolytes have high ionic conductivity and stability, which are composed of a polymer host matrix and a polymer compatible electrolyte [18–22].
In this work, a high scan rate flexible and all solid-state supercapacitor were fabricated using RGO that are decorated via the silver nanoparticles, where silver main function was to prevent RGO self-collapsing /restacking and increase the composite conductivity. Surprisingly, silver enhances the surface area and performance. On the other hand, GP doped with GO and polyaniline played a crucial role in enhancing the scan rate. Phosphoric acid based GP was used due to high performance when used with RGO and extend cell lifetime.

2 Experimental

2.1 Material preparation

All chemicals were purchased from Sigma-Aldrich and used without further purification. GO powder was prepared using improved hummers method [23,24]. After collecting and drying, 1 gram of the GO powder was dispersed in 200 ml of DI water for 2 hours to obtain highly exfoliated graphene oxide using ultrasonic probe. In the meanwhile, 0.5 gram of $AgNO_3$ was dissolved in 25 ml DI water. Two different volume ratio of GO to Ag solution were stirred together for 2h as following (2:50) and (8:50), respectively. After that, the mixture was aged for 6 h. Hydrazine hydrate was used as reduction agent at 95 ^oC in a hot water bath. The participated powder was collated and washed several times with DI water and Ethanol/DI water (50:50) volume ratio. Finally, the collected powder was dried and grinded to be used as the active material that will be defined according to the silver volume ratio as 2ml Ag-RGO and 8ml Ag-RGO. On the other hand, GO was reduced to reduced graphene oxide (RGO) using Hydrazine hydrate in order to apply Raman and XRD analysis and track the dissimilarity.

The gel polymer was prepared by dissolving 10 grams of PVA in 100 ml DI water under reflux at 90 ^oC with 10 grams of H_3PO_4, 6ml of GO suspension and 0.01 g of polyaniline were added then stirred for 6h at RT. Polyaniline was prepared via rapid mixing reaction and dissolved in DMF [25–27].

2.2 Device fabrication

The active material was prepared by adding RGO-Ag/PVDF with a weight ratio of 9:1, respectively. The active material, gel polymer, active material were printed layer after layer manually on the commercial projector plastic film using a glass tube. Total active material weight on a single electrode was 0.01 gram while the electrode area was about 1x4 cm^2. It is worth to mention that, each layer was dried at 60 ^oC in vacuum before applying another layer. Finally, the compact device was peeled off the substrate then a mask was used to deposit 0.5μm of silver thin film on both sides to be used as the charge collectors.

2.3 Characterization

X-ray diffraction (X'Pert pro) and dispersive Raman microscopy (Bruker Senterraa) with a 532 nm laser source having a power of 10 mW were applied. The green laser was focused onto the sample with an optical microscope at lens of 50× magnifications. Transmission electron microscope (HRTEM, JOEL JEM-2100) was used for microscopic investigations. All electrochemical measurements were carried out using a Bio-logic VSP-300 potentiostat /galvanostat. These measurements included cyclic voltammetry (CV), charge-discharge and electrochemical impedance spectroscopy (EIS). The CV tests were carried out at different scan rates ranging from 10 to 200 mV/s, and the electrochemical EIS measurements were conducted in the frequency range from 0.1 Hz to 2 MHz.

3 Result and discussion

XRD pattern of GO, RGO and 8ml Ag-RGO extracted powder is shown in Fig.1 (a). The GO exhibited a distinct narrow peak centered at $2\theta = 11.37^o$ corresponding to an interlayer spacing of the [002] facet equal to d_{002}= 0.775nm, which is exceeding the value of graphene ~0.34

nm [28]. The oxidized GO sheet is reported to incorporate hydrophilic oxygen functional groups such as carbonyl, carboxyl, hydroxyl and epoxy. According to Debye-Scherrer's equation, the estimated crystallite size is ~28.96 nm indicating a fair reduction process. The d-spacing of GO layers was estimated to be ~7.7 Å that is associated with the intercalated water content coupled with highly oxidized GO lattice [29]. On the other hand, RGO revealed an upshifted broad peak at 24.04º reducing the [002] graphitic interlayer spacing to 0.369 nm with much less d spacing than crude GO and near to graphene thickness. Reduction effect on bond cleavage of the inveterate oxygen functional groups in GO contributes to the decomposition of oxygen functional groups and the formation of smaller and dispersed sp^2 hybridized carbon domains [28].

The 8ml Ag-RGO sample showed a number of reflections at 32.2º, 38.12°, 44.28º, 64.5º, and 77.49º corresponding to the (400), (111), (200), (220) and (311) fcc silver facets, respectively [30]. While the other peaks before 30º could be attributed to crystallization of carbon on silver surface. The calculated average particle size of the most dominated peaks of Ag for each plan are presented in table 1. Furthermore, the diffraction peak of RGO red shifted to 25.2º indicating higher reduction degree. The polycrystalline silver and mild high average particle size could be attributed to reduction at 95 ºC that promoted crystallization.

Table 1:

2Θ	**Average grain size**
32.23º	60.4 nm
38.12º	86.2 nm
44.28º	55.4 nm
64.5º	39.9 nm

Fig. 1 Prepared powder of GO, RGO and Ag-RGO. (a). X-ray diffraction and (b). Raman spectra. (c) TEM images of GO and (d) 8ml Ag-RGO.

Raman spectroscopy is the most reliable and non-destructive for graphene-based material [31–35]. Fig. 1 (b) shows Raman spectra of GO film and RGO and 8ml Ag-RGO on glass substrate. Raman peaks of the while spectra are located at

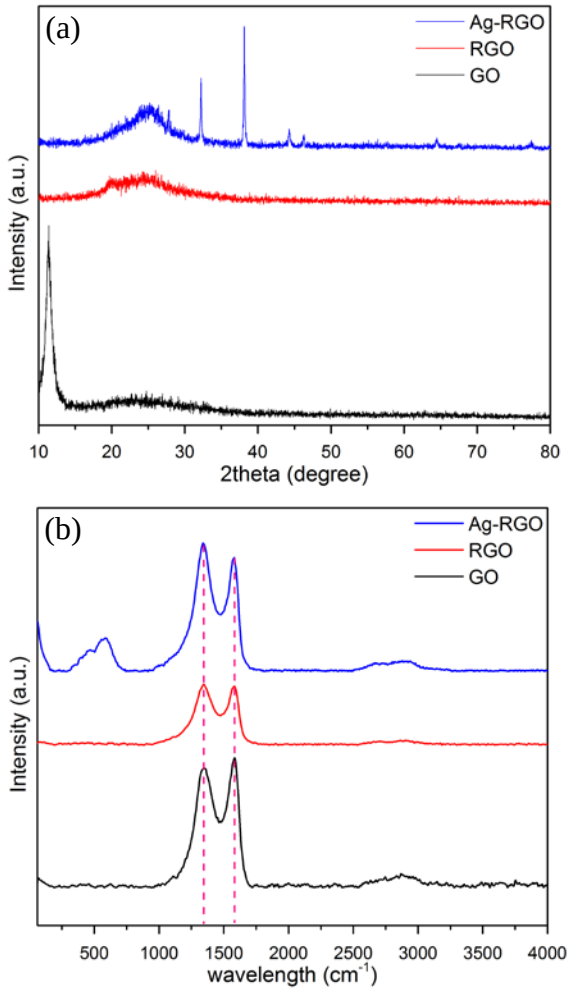

Fig. 1 Prepared powder of GO, RGO and Ag-RGO. (a). X-ray diffraction and (b). Raman spectra. (c) and (d) TEM images of GO and 8ml Ag-RGO.

1345.5 (D), 1584 (G) cm^{-1}, whereas a broad feeble bump is located at the well-defined 2D position, the dashed lines showed that the peaks positions are irrelevant to reduction or decoration process. GO flakes has many defects

caused by aggressive chemical oxidation process. Therefore, RGO would also have those defects in addition to others that are generated during reduction process. On the other hand, Ag reduction process will promote defects formation and disordering even more than the previously mentioned GO, RGO, 8ml Ag-RGO as a result of intercalated Ag inside RGO layers and aggressive reduction process as well. Therefore, this is manifested as an increase in I_D/I_G intensity ratio to be 0.919, 1.03 and 1.11, respectively [36,37]. Although the D and G band location was reserved as the as prepared GO, a broad hump centered at 570 indicate the silver nanoparticles Raman peaks was appeared [30].

Fig. 1 (c) shows the TEM image of GO layer that is clear and appeared to be folded in some parts. But, Fig. 1 (d) presents the silver nanoparticles that are not only cover the layers but also seems to accumulate over each other in semi-spherical shape and appeared as dark spots. In addition, the dark region on the bottom is referring to RGO folded layers.
Fig. 2. (a) Shows a photographic image of the 8ml Ag-RGO SC after printing on the commercial plastic film, whereas Fig. 2 (b) is an image after peeling off and silver deposition as the current collectors. The fabricated devices were flexible, stretchable and lightweight because of the natural form of polymer-based structure. It is worth to mention that, the detailed study of different ratios of Ag to RGO, flexibility, and stretching impact on performance is being published elsewhere.

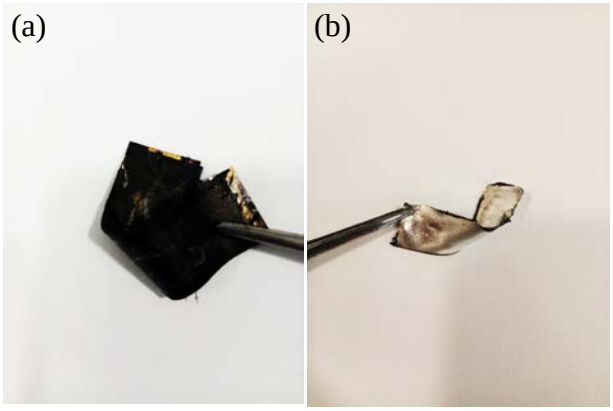

Fig. 2 Digital images of the flexible SCs. (a) on the plastic substrate and (b) after peeling and silver coating.

CV curves at different scan rates starting from 10 mv/sec to 200mv/sec for 2ml Ag-RGO and 8ml Ag-RGO is presented at Fig. 3 (a) and (b), respectively. Therefore, the higher silver weight ratio sample proved superiority in terms of maximum current, CV profile, which indicated a large capacitance variety between the two devices. In addition, the two samples didn't show any peaks or humps that refer to ideal EDL behavior. The quasi-rectangular shape that dominates the two curves could be attributed using the H_3PO_4.

The specific capacitance versus the applied scan rates was calculated using Eq. 1.

$$C = \frac{\int Idv}{mv\Delta V} \quad (1)$$

Where the first term is the area under curve and ΔV is the operation voltage window, v is the scan and m is the total two electrodes active material weight in grams.

The highest specific capacitance values of 2 Ag-RGO and 8 Ag-RGO at 10 mv/sec were 37.5 F/g and 164 F/g, respectively. While the lowest value was achieved at the 200 mV/s.

Table 2 shows the values of capacitances at different scan rates

As the scan rates increase, the expected capacitance would decrease because the limited diffusion of electrolyte ions within the electrode active material and pore, which shrink the electrochemical effective surface area and the cations and anions mobility through the active material [38].

Table2:

Scan rates	2ml	8ml
10 mv/sec	37.5 F/g	164 F/g
20 mv/sec	20 F/g	96.6 F/g
50 mv/sec	10 F/g	51.3 F/g
100 mv/sec	6 F/g	31.57 F/g
200 mv/sec	4.5 F/g	19.24 F/g

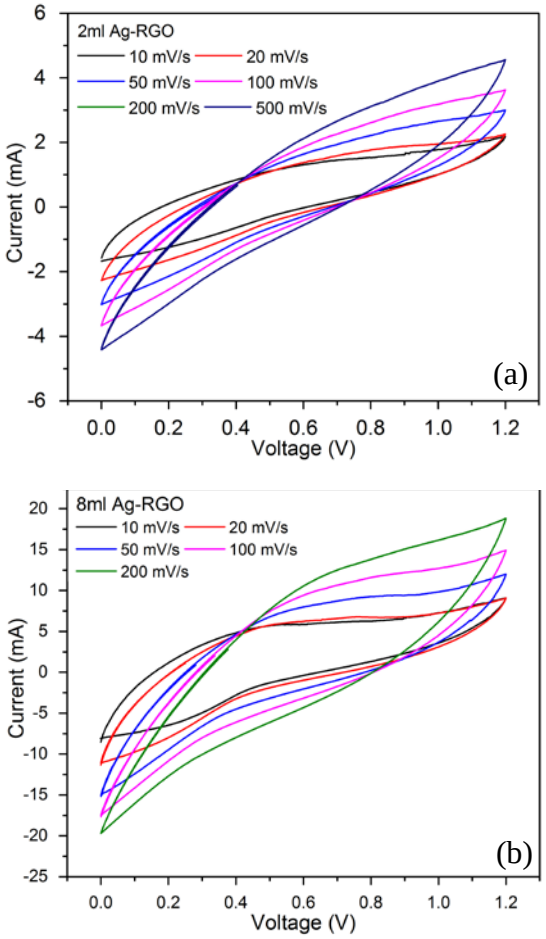

Fig. 3 (a) CV curves at different scan rates from 10 to 200 mv/s. b. (a) 2ml Ag-RGO sample and (b) 8ml Ag-RGO sample.

Galvanostatic charge/discharge electrochemical characterization was performed at 2A in order to force the fabricated devices to work at relatively high current. The first 3 charge/discharge cycles are shown in Fig. 4, where the time scale of the 8 Ag-RGO is about four-fold than the smaller ratio one that is in good agreement with the CV calculations as well. Besides, the small silver ratio sample couldn't withstand the high current rate and fallout to millisecond scale, which promotes the silver nanoparticles crucial impact of the active material performance.

The energy density was calculated using equation 2:

$$E_{cell} = \frac{CsV2}{8} \qquad (2)$$

Where, Cs the specific capacitance, V is the operation voltage and Δt is the discharge time. Therefore, the energy and power densities could be dramatically increased upon using high operation voltage. The maximum energy density of the 8ml Ag-RGO is 29.5 W/Kg. But, the 2ml Ag-RGO was 6.75 W/Kg only.

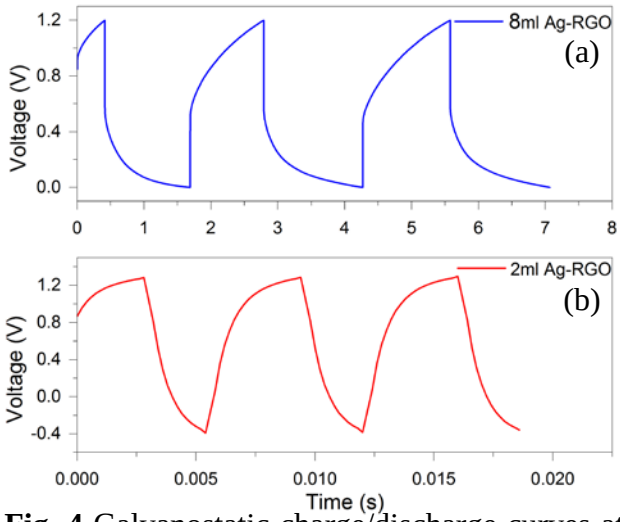

Fig. 4 Galvanostatic charge/discharge curves at 2 A/g. (a) 2ml Ag-RGO sample, (b) 8ml Ag-RGO sample.

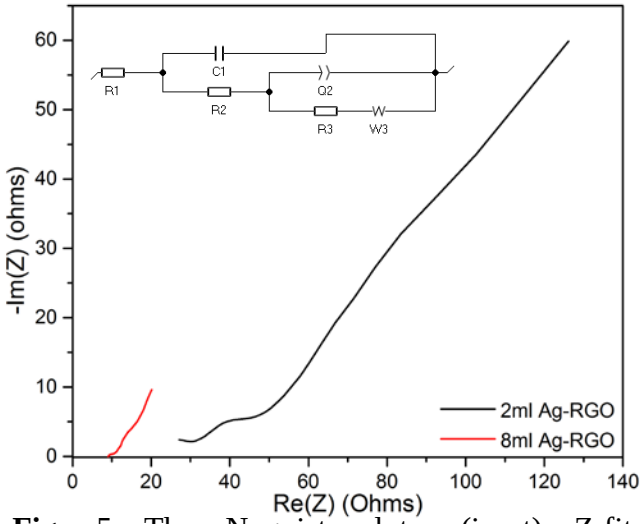

Fig. 5 The Nyquist plots. (inset) Z-fit Equivalent circuit.

EIS characterization for SCs was performed at frequency range from 2MHz to 0.1 Hz. The Nyquist plot exhibits the impedance real part versus imaginary part is presented in Fig. 5, where the equivalent series resistance (ESR) of the electrode can be observed from the x-intercept of the Nyquist plot. The EC-Lab produced Zfit of the equivalent circuit [R1+C1/(R2+Q2/(R3+W3))] (inset Fig. 5)

where Q2 is a constant phase element (CPE). The interpretation of CPE parameters in terms of physically meaningful properties such as capacitance requires an understanding of the nature of the time-constant distribution, where R1 represents charge transfer resistance within electrodes, W3 represents Warburg resistance that mean the resistance of ions diffusion in electrolyte, C1, R2 and R3 represent the resistance and capacitance two electrode. The equivalent series resistance of 2 ML and 8ML were 2.9 and 0.5317 ohms, respectively. Although ESR is small, it could be further enhanced upon using a high mobility ion such as the K^+ [18]. Despite applying easy printing technique, the missing active material compressing step decrease the obtained capacity. In addition, the low resistance region slop behavior is due to phosphoric weak acid natural [39].

4 Conclusion

High performance, half printed, flexible and all-solid-state EDL asymmetric SCs based on silver decorated reduced graphene oxide was fabricated. The silver weight ratio to RGO seems to highly affect the specific capacitance values and performance, as the 8 Ag-RGO attain 164 F/g correlated with using a weak ion based electrolyte. The cooperation of silver nanoparticles seems not to only increase conductivity but also expand surface area and enhance the electrochemical performance. The TEM images proved the silver nanoparticles incorporation on the RGO surface. Whereas, XRD showed the carbon crystallization on the Ag surface. The developed GP by adding GO suspension that promotes ions mobility while polyaniline increase the conductivity. Finally, 0.5 ohm represents the smallest electric series resistance, which would directly affect the power of the all solid-state SCs as the highest achieved energy density is 29.5 W/Kg (at 0.25A).

References:

[1] Winter M., Brodd R.J., What Are Batteries, Fuel Cells, and Supercapacitors? Contents, Chem. Rev. 104, 2004, 4245–4269.

[2] A. González, E. Goikolea, J.A. Barrena, R. Mysyk, Review on supercapacitors: Technologies and materials, Renew. Sustain. Energy Rev. 58, 2016, 1189–1206.

[3] J. Amouroux, P. Siffert, J. Pierre Massué, S. Cavadias, B. Trujillo, K. Hashimoto, P. Rutberg, S. Dresvin, X. Wang, Carbon dioxide: A new material for energy storage, Prog. Nat. Sci. Mater. Int. 24, 2014, 295–304.

[4] M. Vangari, T. Pryor, L. Jiang, Supercapacitors: Review of Materials and Fabrication Methods, J. Energy Eng. 139, 2012, 72–79.

[5] P. Simon, Y. Gogotsi, Materials for electrochemical capacitors, Nat. Mater. 7, 2008, 845–854.

[6] K.S. Novoselov, V.I. Fal'ko, L. Colombo, P.R. Gellert, M.G. Schwab, K. Kim, A roadmap for graphene, Nature. 490, 2012, 192–200.

[7] M. Liang, L. Zhi, Graphene-based electrode materials for rechargeable lithium batteries, J. Mater. Chem. 19, 2009, 5871–5878.

[8] J. Luo, H.D. Jang, J. Huang, Effect of sheet morphology on the scalability of graphene-based ultracapacitors, ACS Nano. 7, 2013, 1464–1471.

[9] R.S.R. Yanwu Zhu, Shanthi Murali, Meryl D. Stoller, K. J. Ganesh, Weiwei Cai, Paulo J. Ferreira, Adam Pirkle, Robert M. Wallace, Katie A. Cychosz, Matthias Thommes, Dong Su, Eric A. Stach, Carbon-Based Supercapacitors Produced by the Activation of Graphene, Science. 332, 2011, 1537–1541.

[10] C. Yang, J. Shen, C. Wang, H. Fei, H. Bao, G. Wang, All-solid-state asymmetric supercapacitor based on reduced graphene oxide/carbon nanotube and carbon fiber paper/polypyrrole electrodes, J. Mater. Chem. A. 2, 2014, 1458–1464.

[11] G. Wang, L. Zhang, J. Zhang, A review of electrode materials for electrochemical supercapacitors, Chem. Soc. Rev. 41, 2012, 797–828.

[12] A. Nag, A. Mitra, S.C. Mukhopadhyay, Graphene and its sensor-based applications: A review, Sensors Actuators, A Phys. 270, 2018, 177–194.

[13] M. Kaur, M. Kaur, V.K. Sharma, Nitrogen-doped graphene and graphene quantum dots: A review onsynthesis and applications in energy, sensors and environment, Adv. Colloid Interface Sci. 259, 2018, 44–64.

[14] Y.J. Kang, H. Chung, C.H. Han, W. Kim, All-solid-state flexible supercapacitors based on papers coated with carbon nanotubes and

ionic-liquid-based gel electrolytes, Nanotechnology. 23, 2012, 289501–6.

[15] X. Jian, H. min Yang, J. gang Li, E. hui Zhang, L. le Cao, Z. hai Liang, Flexible all-solid-state high-performance supercapacitor based on electrochemically synthesized carbon quantum dots/polypyrrole composite electrode, Electrochim. Acta. 228, 2017, 483–493.

[16] A. Lamberti, M. Fontana, S. Bianco, E. Tresso, Flexible solid-state CuxO-based pseudo-supercapacitor by thermal oxidation of copper foils, Int. J. Hydrogen Energy. 41, 2016, 11700–11708.

[17] X. Lu, M. Yu, G. Wang, Y. Tong, Y. Li, Flexible solid-state supercapacitors: Design, fabrication and applications, Energy Environ. Sci. 7, 2014, 2160–2181.

[18] F. Barzegar, J.K. Dangbegnon, A. Bello, D.Y. Momodu, A.T.C. Johnson, N. Manyala, Effect of conductive additives to gel electrolytes on activated carbon-based supercapacitors, AIP Adv. 5, 2015, 097171-9.

[19] X. Yang, F. Zhang, L. Zhang, T. Zhang, Y. Huang, Y. Chen, A high-performance graphene oxide-doped ion gel as gel polymer electrolyte for all-solid-state supercapacitor applications, Adv. Funct. Mater. 23, 2013, 3353–3360.

[20] Q. Chen, X. Li, X. Zang, Y. Cao, Y. He, P. Li, K. Wang, J. Wei, D. Wu, H. Zhu, Effect of different gel electrolytes on graphene-based solid-state supercapacitors, RSC Adv. 4, 2014, 36253–36256.

[21] U.N. Maiti, J. Lim, K.E. Lee, W.J. Lee, S.O. Kim, Three-dimensional shape engineered, interfacial gelation of reduced graphene oxide for high rate, large capacity supercapacitors, Adv. Mater. 26, 2014, 615–619.

[22] X. Yang, L. Zhang, F. Zhang, T. Zhang, Y. Huang, Y. Chen, A high-performance all-solid-state supercapacitor with graphene-doped carbon material electrodes and a graphene oxide-doped ion gel electrolyte, Carbon N. Y. 72, 2014, 381–386.

[23] C. Botas, P. Álvarez, C. Blanco, R. Santamaría, M. Granda, P. Ares, F. Rodríguez-Reinoso, R. Menéndez, The effect of the parent graphite on the structure of graphene oxide, Carbon. 50, 2012, 275–282.

[24] W.S. Hummers, R.E. Offeman, Preparation of Graphitic Oxide, J. Am. Chem. Soc. 80, 1958, 1339–1339.

[25] J. Huang, S. Virji, B.H. Weiller, R.B. Kaner, Nanostructured Polyaniline Sensors, Chem. - A Eur. J. 10, 2004, 1314–1319.

[26] L.I. Dan, J. Huang, R.B. Kaner, Polyaniline nanofibers: a unique polymer nanostructure for versatile applications, Acc. Chem. Res. 42, 2009, 135–145.

[27] K. Zhang, L.L. Zhang, X.S. Zhao, J. Wu, Graphene/polyaniline nanofiber composites as supercapacitor electrodes, Chem. Mater. 22, 2010, 1392–1401.

[28] S. Stankovich, D.A. Dikin, R.D. Piner, K.A. Kohlhaas, A. Kleinhammes, Y. Jia, Y. Wu, S.B.T. Nguyen, R.S. Ruoff, Synthesis of graphene-based nanosheets via chemical reduction of exfoliated graphite oxide, Carbon. 45, 2007, 1558–1565.

[29] H. Jeong, Y.P. Lee, R.J.W.E. Lahaye, M. Park, K.H. An, I.J. Kim, C. Yang, C.Y. Park, R.S. Ruoff, Y.H. Lee, Evidence of Graphitic AB Stacking Order of Graphite Oxides, J. AM. CHEM. SOC. 2008, 155–158.

[30] S. Sang, D. Li, H. Zhang, Y. Sun, A. Jian, Facile synthesis of AgNPs on reduced graphene oxide for highly sensitive simultaneous detection, RSC Adv. 7, 2017, 21618–21624.

[31] A. Ferrari, D. Basko, Raman spectroscopy as a versatile tool for studying the properties of graphene, Nat. Nanotechnol. 8, 2013, 235–46.

[32] A.C. Ferrari, J.C. Meyer, V. Scardaci, C. Casiraghi, M. Lazzeri, F. Mauri, S. Piscanec, D. Jiang, K.S. Novoselov, S. Roth, A.K. Geim, Raman spectrum of graphene and graphene layers, Phys. Rev. Lett. 97, 2006, 1–4.

[33] A. Elhamid, M.A. Elhamid, M.A. Hafez, A.M. Aboulfotouh, I.M. Azzouz, temperature Study of graphene growth on copper foil by pulsed laser deposition at reduced temperature, J. Appl. Phys. 025303, 2017, 1–7.

[34] A.M. Abd Elhamid, A.M. Aboulfotouh, M.A. Hafez, I.M. Azzouz, Room temperature graphene growth on complex metal matrix by PLD, Diam. Relat. Mater. 80, 2017, 162–167.

[35] I.M.A. A.M. Abd Elhamid, A. M. Hafez, A.M. Aboulfotouh, Study of graphene growth on Copper Foil by Pulsed Laser Deposition at Reduced Temperature, J. Appl. Phys. 121, 2017, 025303-7.

[36] I.K. Moon, J. Lee, R.S. Ruoff, H. Lee, Reduced graphene oxide by chemical

graphitization, Nat. Commun. 1, 2010, 1–6.

[37] A. Vianelli, A. Candini, E. Treossi, V. Palermo, M. Affronte, Observation of different charge transport regimes and large magnetoresistance in graphene oxide layers, Carbon N. Y. 89, 2015, 188–196.

[38] N. Mishra, S. Shinde, R. Vishwakarma, S. Kadam, M. Sharon, M. Sharon, MWCNTs synthesized from waste polypropylene plastics and its application in super-capacitors, AIP Conf. Proc. 1538, 2013, 228–236.

[39] V.A. Online, Q. Chen, X. Li, X. Zang, Y. Cao, Y. He, P. Li, K. Wang, J. Wei, D. Wu, H. Zhu, Effect of different gel electrolytes on graphene- based solid-state supercapacitors, RSC Adv. 36253, 2014, 36253–36256.